Available online at www.sciencedirect.com
ScienceDirect
Ceramics International 34 (2008) 883–888
CERAMICS INTERNATIONAL
www.elsevier.com/locate/ceramint

Relationships between crystal structure and microwave dielectric properties of $(Zn_{1/3}B_{2/3}^{5+})_xTi_{1-x}O_2$ (B^{5+} = Nb, Ta) ceramics

Eung Soo Kim *, Dong Ho Kang

Department of Materials Engineering, Kyonggi University, Suwon 443-760, Republic of Korea

Available online 29 September 2007

Abstract

Dependence of microwave dielectric properties on the crystal structure of $(Zn_{1/3}B_{2/3}^{5+})_xTi_{1-x}O_2$ (B^{5+} = Nb, Ta) ceramics was investigated as a function of $Zn_{1/3}B_{2/3}^{5+}O_2$ (B^{5+} = Nb, Ta) content ($0.4 \leq x \leq 0.7$). Dielectric constant (K) and the temperature coefficient of resonant frequency (TCF) of sintered specimens were strongly dependent on the structural characteristics of oxygen octahedra in rutile structure. Cation rattling and the distortion of oxygen octahedra were dependent on the bond length ratio of apical (d_{apical})/equatorial ($d_{equatorial}$) of oxygen octahedra. The quality factor (Qf) was dependent on the reduction of Ti ion as well as the microstructure of the sintered specimens.

Keywords: A. Sintering; C. Dielectric properties; D. TiO_2; Octahedral distortion

1. Introduction

Microwave dielectric properties are affected by the crystal structure and the interactions between cation and anion of the compound. At microwave frequencies, the dielectric constant was found to be affected by the rattling effect as well as the dielectric polarizability, and the temperature coefficient of resonant frequency was closely related with the temperature coefficient of dielectric constant (TCK), which is depended on the distortion of oxygen octahedral [1]. On the other hand, the rattling effect and the octahedral distortion were largely dependent on the bond strength and bond length of the composing ions.

It has been reported [2] that Ti^{4+} ions of TiO_2 can be substituted by Nb^{5+} or Ta^{5+} as well as monovalent, divalent, or trivalent cation. The extensive new rutile solid solutions of $(A_{1/3}^{2+}B_{2/3}^{5+})_xTi_{1-x}O_2$ have been prepared in which Ti^{4+} was replaced by a divalent and a pentavalent cation. The substitution of Ti^{4+} ions of TiO_2 by other ions would affect the microwave dielectric properties and the crystal structures of the specimens. The ionic size differences between Zn^{2+} ion (0.74 Å), Nb^{5+} ion (0.64 Å) and/or Ta^{5+} ion (0.64 Å) and Ti^{4+} ion (0.605 Å) are not much at the same coordination number (C.N. = 6) [3]. Therefore, tetravalent Ti^{4+} ion in the TiO_2 could be substituted by one third of Zn^{2+} ion and two third of Nb^{5+} and/or Ta^{5+} ions for the charge compensating.

In the rutile structure, the cation is coordinated to six oxygen ions and each oxygen ion is coordinated to three cations. These octahedra form chains, cross-linked by sharing corners at each cation–oxygen bond. The TiO_6 octahedra in rutile TiO_2 consisted of four equatorial Ti–O bonds and two apical Ti–O bonds, is slightly distorted with longer apical Ti–O bonds slightly than the other equatorial bond [4]. The distortion of the oxygen octahedral surrounding each Ti atom is decided by the oxygen position parameter u, the axial ratio c/a, and lattice parameter of a-axis. As to solid solutions between TiO_2 and $Zn_{1/3}B_{2/3}^{5+}O_2$ (B^{5+} = Nb, Ta), the octahedral distortion should be changed with the compositional variations of $(Zn_{1/3}B_{2/3}^{5+})_xTi_{1-x}O_2$.

In this study, the microwave dielectric properties and crystal structure of the $(Zn_{1/3}B_{2/3}^{5+})_xTi_{1-x}O_2$ (B^{5+} = Nb, Ta) system were investigated as a function of the amount of $Zn_{1/3}B_{2/3}^{5+}O_2$ (B^{5+} = Nb, Ta) ($0.4 \leq x \leq 0.7$). Dependence of dielectric constant on the rattling effects and the dependence of TCF on the octahedral distortion of oxygen octahedra were also discussed.

2. Experimental procedure

ZnO, Nb_2O_5, Ta_2O_5, and TiO_2 powders with reagent-grade were used as starting materials. They were weighed

* Corresponding author. Tel.: +82 31 249 9764; fax: +82 31 244 6300.
E-mail address: eskim@kyonggi.ac.kr (E.S. Kim).

0272-8842/$34.00
doi:10.1016/j.ceramint.2007.09.049

according to the compositions of $ZnB_2^{5+}O_6$ (B^{5+} = Nb, Ta), and then milled with ZrO_2 balls for 24 h in distilled water. Powders with a composition of $ZnNb_2O_6$ and/or $ZnTa_2O_6$ were calcined at 900 °C and/or 1200 °C for 3 h, respectively. These calcined powders were mixed according to the formula of $(Zn_{1/3}B_{2/3}^{5+})_xTi_{1-x}O_2$ (B^{5+} = Nb, Ta, $0.4 \leq x \leq 0.7$). Mixtures with B^{5+} = Nb and/or Ta were calcined at 1100 °C and/or 1200 °C for 3 h, respectively. The calcined powders were milled again with ZrO_2 balls for 24 h in distilled water and then dried. The dried powders were pressed into 10 mm diameter disk at 1500 kg/cm^2 isostatically. These pellets were sintered from 1050 °C to 1250 °C for 3 h in air. The heating rate was 5 °C/min and the cooling rate was 1 °C/min down to 900 °C, and then furnace cooled to room temperature.

Crystalline phases of the specimens were identified with the powder X-ray diffraction patterns (D/Max-3C, Rigaku, Japan). The sintered specimens was pulverized and weighted with a 10 wt.% of internal standard Si powder to correct 2θ. From the Rietveld refinements of X-ray diffraction patterns, the lattice parameters and unit cell volume of the sintered specimens were determined. Microstructure was observed using a scanning electron microscope and energy dispersive spectrometer (JEOL, JSM-6500F). The dielectric constant, unloaded Q value at frequencies of 5–7 GHz was measured by the post-resonant method developed by Hakki and Coleman [5]. *TCF* was measured by the cavity method [6] at the temperature range of 25–80 °C.

From the lattice parameters and oxygen position parameter of tetragonal rutile structure, the individual bond length [7] of oxygen octahedral was obtained from Eqs. (1)–(3):

$$d_{\text{apical}} = au\sqrt{2} \tag{1}$$

$$d_{\text{equatorial}} = 0.5a\left[2(2u-1)^2 + \left(\frac{c}{a}\right)^2\right]^{1/2} \tag{2}$$

$$u = \frac{2 - (4 - 2(1 - (d_{\text{equatorial}}/d_{\text{apical}})^2)((c/a)^2 + 2))^{1/2}}{4(1 - (d_{\text{equatorial}}/d_{\text{apical}})^2)} \tag{3}$$

where a and c are the lattice parameters and u is the oxygen position parameter in oxygen octahedral. From the individual bond length of oxygen octahedra, the octahedral distortion (Δ) was calculated in Eq. (4) [3]:

$$\Delta = \frac{1}{6}\sum\left\{\frac{R_i - \bar{R}}{\bar{R}}\right\}^2 \tag{4}$$

where R_i is the individual bond length and $\bar{R}$ is the average bond length of oxygen octahedral, respectively.

3. Results and discussion

Fig. 1 shows the X-ray diffraction patterns of $(Zn_{1/3}B_{2/3}^{5+})_xTi_{1-x}O_2$ (B^{5+} = Nb, Ta) sintered specimens. The specimens with B^{5+} = Nb and/or B^{5+} = Ta were sintered at 1100 °C and/or 1200 °C for 3 h, respectively. For the specimens with $Zn_{1/3}Ta_{2/3}O_2$, tetragonal rutile solid solutions were obtained through the entire composition, while the ixiolite $ZnTiNb_2O_8$ was detected as a secondary phase of $(Zn_{1/3}Nb_{2/3})_{0.7}Ti_{0.3}O_2$, along with rutile phase, and these solid solution limits depend on substituted B^{5+} ion [8]. Fig. 2 shows the crystal structure of rutile solid solution. In the $(Zn_{1/3}B_{2/3}^{5+})_xTi_{1-x}O_2$ (B^{5+} = Nb, Ta) system, the Zn^{2+} and B^{5+} cations are substituted into the rutile structure, and then distributed at random over the octahedral Ti^{4+} sites [2].

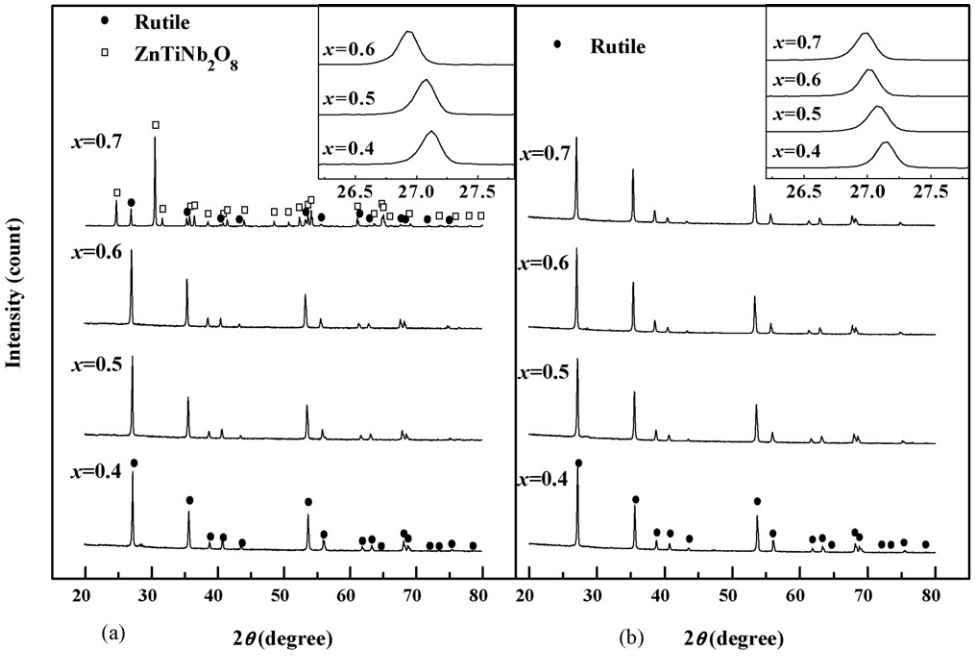

Fig. 1. X-ray diffraction patterns of $(Zn_{1/3}B_{2/3}^{5+})_xTi_{1-x}O_2$ ($0.4 \leq x \leq 0.7$) sintered specimens: (a) B^{5+} = Nb and (b) B^{5+} = Ta.

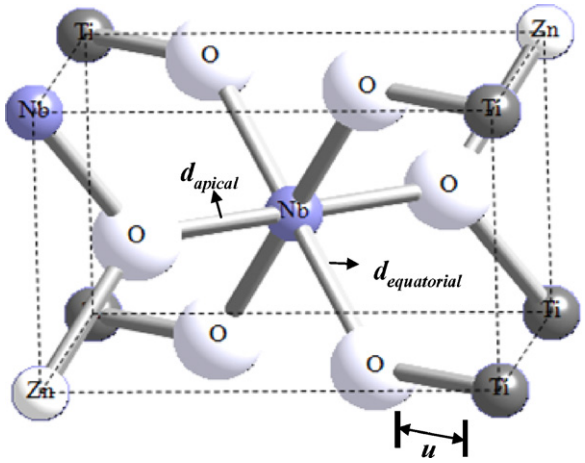

Fig. 2. Crystal structure of rutile solid solution $(Zn_{1/3}Nb_{2/3})_{0.5}Ti_{0.5}O_2$.

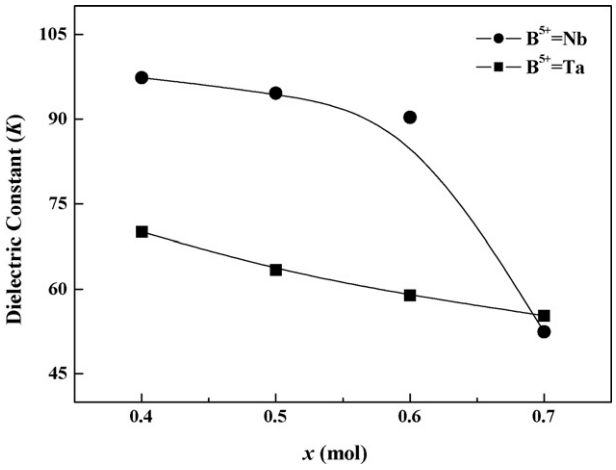

Fig. 3. Dielectric constant (K) of $(Zn_{1/3}B_{2/3}^{5+})_xTi_{1-x}O_2$ sintered specimens.

Crystallographic data obtained from a Rietveld refinement for $(Zn_{1/3}B_{2/3}^{5+})_xTi_{1-x}O_2$ (B^{5+} = Nb, Ta) are summarized in Table 1. With an increase of $Zn_{1/3}B_{2/3}^{5+}O_2$ (B^{5+} = Nb, Ta) content, the peaks in XRD patterns shifted to lower angle, as shown in the inserts of Fig. 1. This indicated that unit-cell volume of solid solution increased with $Zn_{1/3}B_{2/3}^{5+}O_2$ (B^{5+} = Nb, Ta) content, as shown in Table 1. These results could be explained by the change of average ionic radius with $Zn_{1/3}B_{2/3}^{5+}O_2$ content due to the larger ionic radius of Zn^{2+} (0.74 Å), Nb^{5+} (0.64 Å) and Ta^{5+} (0.64 Å) than that of Ti^{4+} (0.605 Å) at same coordination number, C.N. = 6 [3].

Dielectric constant (K) of $(Zn_{1/3}B_{2/3}^{5+})_xTi_{1-x}O_2$ (B^{5+} = Nb, Ta) sintered specimens is shown in Fig. 3. Within the solid solution range, K of the specimens decreased linearly with $Zn_{1/3}B_{2/3}^{5+}O_2$ (B^{5+} = Nb, Ta) content, while that of $(Zn_{1/3}Nb_{2/3})_{0.7}Ti_{0.3}O_2$ decreased drastically due to the smaller K of $ZnTiNb_2O_8$ [9] than that of rutile solid solution, Also effects of density on the dielectric constant could be neglected because the relative density of the specimens was larger than 93% of X-ray density.

Rutile compounds are characterized by extended apical bonds, and bond length ratio of apical (d_{apical})/equatorial ($d_{equatorial}$) leading to rattling cations in rutile structure. Apical bond lengths of TiO_2 with rutile structure were extended by 1.6% relative to the equatorial bond lengths [10]. Therefore, high dielectric constant (K = 105) of TiO_2 are resulted from apical extension leading to the increase of 'rattling space' by

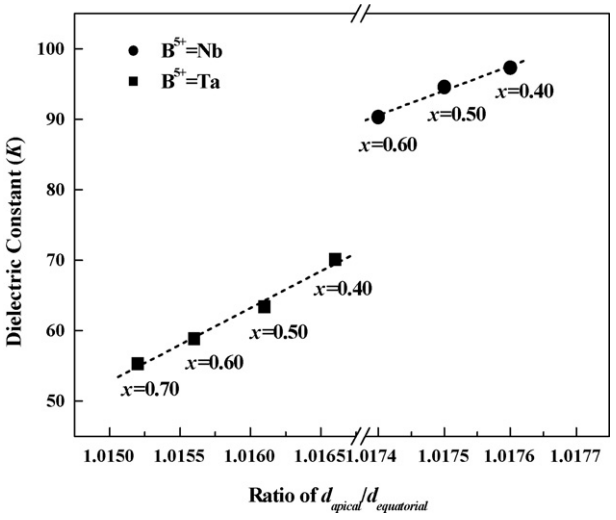

Fig. 4. Dependence of dielectric constant (K) on ratio of $d_{apical}/d_{equatorial}$ of $(Zn_{1/3}B_{2/3}^{5+})_xTi_{1-x}O_2$ sintered specimens.

apical direction within the oxygen octahedron. While the ratio of bond lengths ($d_{apical}/d_{equatorial}$) of SnO_2 with same rutile structure is nearly equal to unity which, in turn, SnO_2 shows a low dielectric constant (K = 12.4), even though the unit cell volume of SnO_2 (71.53 $Å^3$) is larger than TiO_2 (62.42 $Å^3$) [11] and the dielectric polarizability of SnO_2 (6.84 Å) is smaller

Table 1
Crystallographic data obtained from a Rietveld refinement for $(Zn_{1/3}B_{2/3}^{5+})_xTi_{1-x}O_2$ sintered specimens

B^{5+} ion	x (mol)	Lattice parameters (Å)		Tetragonality (c/a)	$V_{unit\ cell}$ ($Å^3$)	u
		a	c			
Nb	0.40	4.6466	3.0038	0.6465	64.8547	0.3054
	0.50	4.6610	3.0165	0.6472	65.5332	0.3055
	0.60	4.6792	3.0321	0.6480	66.3876	0.3057
Ta	0.40	4.6392	3.0032	0.6474	64.6357	0.3054
	0.50	4.6504	3.0158	0.6485	65.2204	0.3055
	0.60	4.6658	3.0314	0.6497	65.9926	0.3056
	0.70	4.6779	3.0437	0.6507	66.6045	0.3057

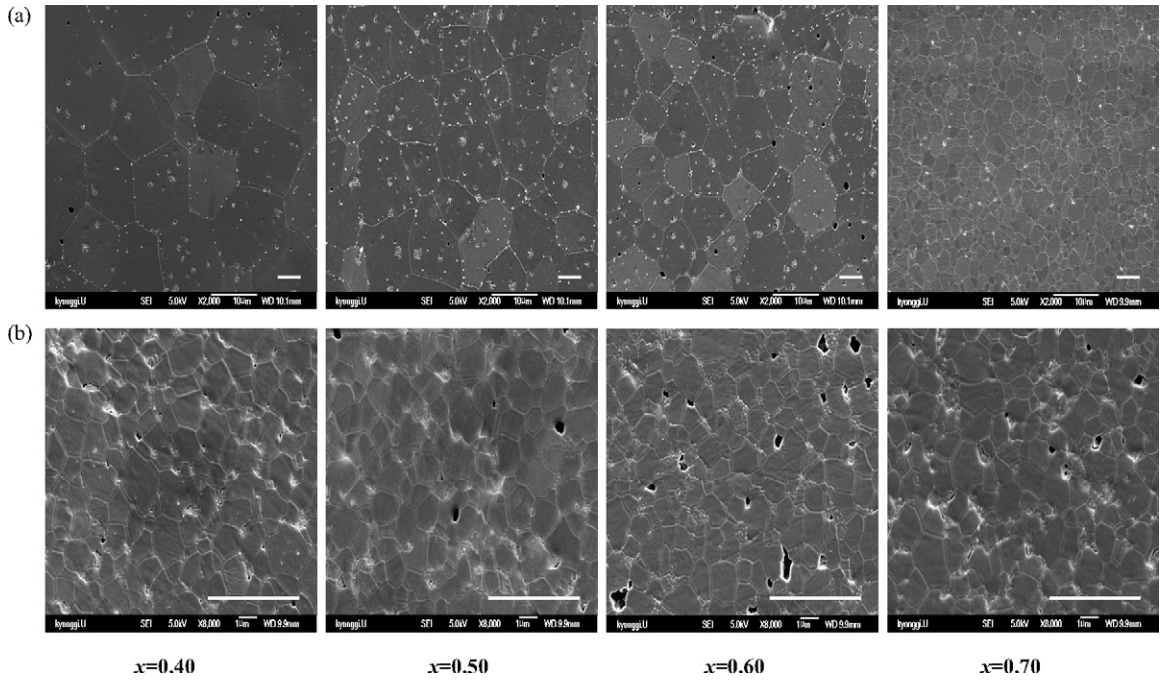

Fig. 5. SEM micrographs of $(Zn_{1/3}B_{2/3}^{5+})_xTi_{1-x}O_2$ sintered specimens: (a) B^{5+} = Nb and (b) B^{5+} = Ta. Bar = 5 μm.

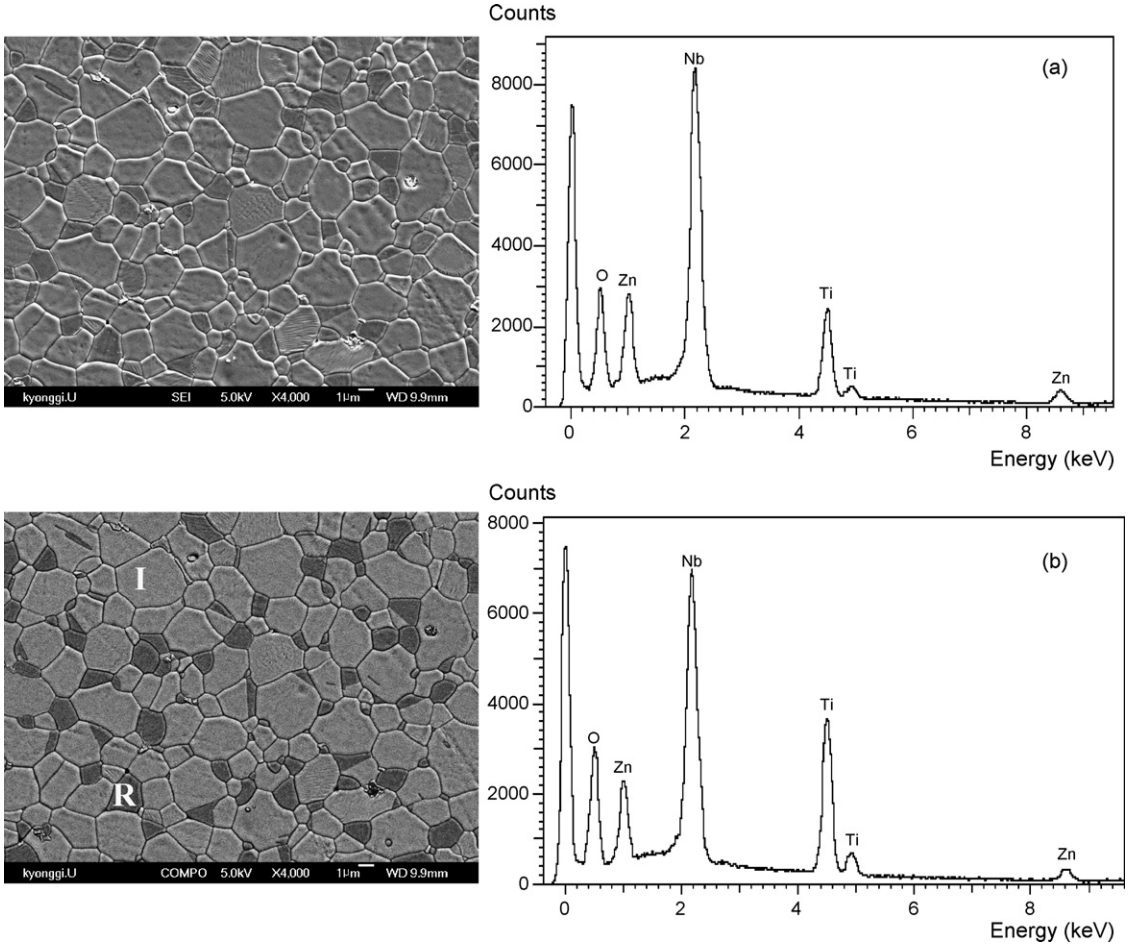

Fig. 6. Back-scattered electron images of $(Zn_{1/3}Nb_{2/3})_{0.7}Ti_{0.3}O_2$ specimens sintered at 1100 °C for 3 h: (a) phase I and (b) phase R. Bar = 5 μm.

Table 2
EDS results of $(Zn_{1/3}Nb_{2/3})_{0.7}Ti_{0.3}O_2$ specimens sintered at 1100 °C for 3 h

Grain I			Grain E		
Element	Element (%)	Atomic (%)	Element	Element (%)	Atomic (%)
O	36.82	72.81	O	39.47	73.43
Ti	12.05	7.96	Ti	19.44	12.08
Zn	12.66	6.13	Zn	9.85	4.49
Nb	38.48	13.10	Nb	31.24	10.01

than TiO_2 (6.95 Å) obtained from the additivity rule of the dielectric polarizability and the ionic polarizabilities (Sn^{4+} = 2.83 Å, Ti^{4+} = 2.93 Å, O^{2-} = 2.01 Å) [12].

Based on these considerations, the decrease in *K* of the $(Zn_{1/3}B_{2/3}^{5+})_xTi_{1-x}O_2$ (B^{5+} = Nb, Ta) ceramics with $Zn_{1/3}B_{2/3}^{5+}O_2$ could be explained by the decrease of cation rattling. With an increasing *x*, the dielectric constants of all prepared specimens are proportional to $d_{apical}/d_{equatorial}$, as shown in Fig. 4. Moreover, *K* of $(Zn_{1/3}Nb_{2/3}^{5+})_xTi_{1-x}O_2$ solid solution was larger than that of $(Zn_{1/3}Ta_{2/3}^{5+})_xTi_{1-x}O_2$ for same *x*. It could be explained that the damped ionic mobility of massive Ta^{5+} ion [13] give rise to weaker interactions with the microwave field, even though the ionic polarizability of Ta^{5+} ion (4.73 Å) is large than that of Nb^{5+} ion (3.97 Å).

Fig. 5 shows SEM micrographs of $(Zn_{1/3}B_{2/3}^{5+})_xTi_{1-x}O_2$ (B^{5+} = Nb, Ta) sintered specimens. The grain size of the specimens with $Zn_{1/3}Nb_{2/3}O_2$ decreased slightly with $Zn_{1/3}Nb_{2/3}O_2$ content up to 0.6 mol, and then decreased remarkably for further addition. However, the specimens with $Zn_{1/3}Ta_{2/3}O_2$ showed smaller grain size than that of the specimens with $Zn_{1/3}Nb_{2/3}O_2$. To confirm the secondary phase of $(Zn_{1/3}Nb_{2/3})_{0.7}Ti_{0.3}O_2$, the back-scattered electron images were observed and EDS analysis was performed, as shown in Fig. 6 and Table 2. From the EDS results, the rutile solid solution phase (R) and ixiolite $ZnTiNb_2O_8$ phase (I) were detected for $(Zn_{1/3}Nb_{2/3}^{5+})_{0.7}Ti_{0.3}O_2$. This result was agreed with XRD patterns of Fig. 1.

Fig. 7 shows the quality factor (*Qf*) of $(Zn_{1/3}B_{2/3}^{5+})_xTi_{1-x}O_2$ (B^{5+} = Nb, Ta) sintered specimens. *Qf* of the specimens with $Zn_{1/3}Nb_{2/3}O_2$ slightly decreased with $Zn_{1/3}Nb_{2/3}O_2$ content up to *x* = 0.6 due to the decrease of grain size, and then increased remarkably due to $ZnTiNb_2O_8$ [9], which has a larger *Qf* value than that of solid solution. However *Qf* of the

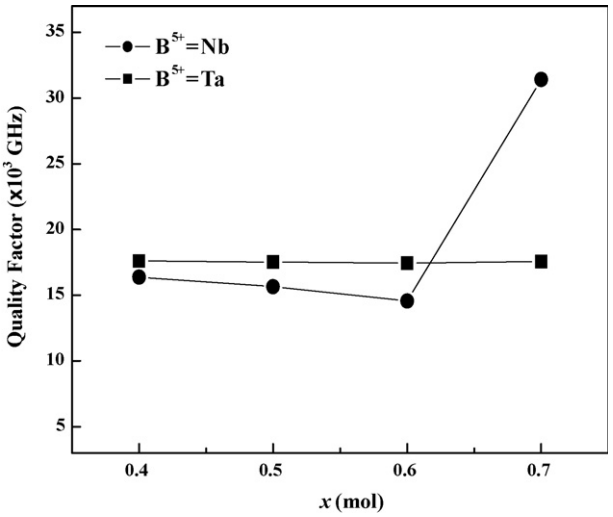

Fig. 7. Quality factor (*Qf*) of $(Zn_{1/3}B_{2/3}^{5+})_xTi_{1-x}O_2$ sintered specimens.

specimens with $Zn_{1/3}Ta_{2/3}O_2$ did not changed with $Zn_{1/3}Ta_{2/3}O_2$ content because there was no difference in the grain size and no detection of secondary phase. In general, microwave dielectric loss was mainly dominated by secondary phase, grain sizes and densification. Although the specimens with $Zn_{1/3}Nb_{2/3}O_2$ showed large grain size and smaller pore than that with $Zn_{1/3}Ta_{2/3}O_2$, *Qf* of the specimens with $Zn_{1/3}Nb_{2/3}O_2$ was smaller than that of $Zn_{1/3}Ta_{2/3}O_2$.

For the sintered specimens with $Zn_{1/3}Nb_{2/3}O_2$, dark gray in color appeared inside the specimens, while the sintered specimens with $Zn_{1/3}Ta_{2/3}O_2$ showed bright yellow in color. It was related to the reduction of Ti^{4+} ion observed frequently in titanium-containing ceramics, due to the small amounts of Ti^{3+} and oxygen vacancies formed during processing [14]. Although there is only a very limited reduction of the TiO_2, the reduction is sufficient to cause a severe deterioration of *Qf* value. Therefore, the differences in quality factor (*Qf*) of $(Zn_{1/3}Nb_{2/3})_xTi_{1-x}O_2$ and $(Zn_{1/3}Ta_{2/3})_xTi_{1-x}O_2$ are associated with the reduction of Ti^{4+}.

The temperature coefficient of resonant frequency (*TCF*) is strongly depended on the structure characteristics of oxygen octahedra such as the bond length between octahedral cation and oxygen ion, and the distortion of oxygen octahedral [1]. For the rutile type structure, there is a close relation between tetragonality (*c*/*a*) and oxygen position parameter (*u*). A critical

Table 3
Octahedral distortion and *TCF* of $(Zn_{1/3}B_{2/3})_xTi_{1-x}O_2$ sintered specimens

B^{5+} ion	*x* (mol)	Bond length (Å)			Distortion ($\Delta \times 10^5$)	*TCF* (ppm/°C)
		d_{apical}	$d_{equatorial}$	$d_{average}$		
Nb	0.40	2.0072	1.9724	1.9840	6.8361	250.13
	0.50	2.0140	1.9794	1.9909	6.7383	237.25
	0.60	2.0227	1.9880	1.9996	6.6846	218.06
Ta	0.40	2.0038	1.9710	1.9819	6.0911	137.61
	0.50	2.0091	1.9774	1.9880	5.6706	97.92
	0.60	2.0165	1.9856	1.9959	5.3336	64.12
	0.70	2.0223	1.9921	2.0022	5.0761	29.87

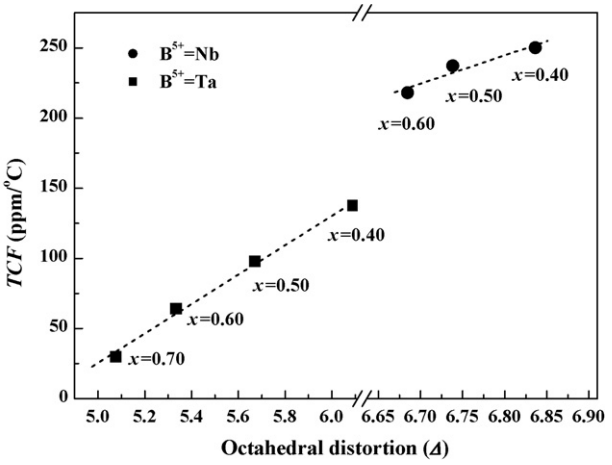

Fig. 8. Dependence of *TCF* on octahedral distortion of $(Zn_{1/3}B_{2/3}{}^{5+})_xTi_{1-x}O_2$ sintered specimens.

value of u is obtained ($u_{cry} = (1/4)[1 + (1/2)(c/a)^2]$) [15] if apical and equatorial bond lengths are equal. When Ti^{4+} ion (0.605 Å) in TiO_2 is substituted by Zn^{2+} ion (0.74 Å), Nb^{5+} ion (0.64 Å) and/or Ta^{5+} ion (0.64 Å), the oxygen octahedron is extended and the change of bond lengths is occurred. Therefore, the distortion from ideal octahedral symmetry ($u = u_{cry}$) results in the changes of apical bond lengths as well as equatorial bond lengths.

Table 3 summarized the oxygen octahedral distortion and *TCF* of $(Zn_{1/3}B_{2/3}{}^{5+})_xTi_{1-x}O_2$ (B^{5+} = Nb, Ta) ceramics obtained from Eqs. (1), (2) and (4). The dependence of thermal stability (*TCF*) on the octahedral distortion of $(Zn_{1/3}B_{2/3}{}^{5+})_xTi_{1-x}O_2$ (B^{5+} = Nb, Ta) ceramics is shown in Fig. 8. With an increase of $Zn_{1/3}B_{2/3}{}^{5+}O_2$ (B^{5+} = Nb, Ta) content, *TCF* of $(Zn_{1/3}B_{2/3}{}^{5+})_xTi_{1-x}O_2$ (B^{5+} = Nb, Ta) ceramics decreased due to the decrease of the octahedral distortion of rutile structure. *TCF* of the specimens with $Zn_{1/3}Ta_{2/3}O_2$ showed smaller value and larger changes with $Zn_{1/3}Ta_{2/3}O_2$ content than that of $Zn_{1/3}Nb_{2/3}O_2$ due to the dampening of *TCK* with Ta substitution [13].

4. Conclusions

The dependence of microwave dielectric properties on the structural characteristics of $(Zn_{1/3}B_{2/3}{}^{5+})_xTi_{1-x}O_2$ (B^{5+} = Nb, Ta) was investigated. For the $(Zn_{1/3}B_{2/3}{}^{5+})_xTi_{1-x}O_2$ (B^{5+} = Nb, Ta, $0.4 \leq x \leq 0.7$) system, a single phase with tetragonal rutile structure was detected up to $x = 0.7$ of B^{5+} = Ta and/or $x = 0.6$ of B^{5+} = Nb, respectively. For the solid solution range, the dielectric constant (K) and the temperature coefficient of resonant frequency (*TCF*) of $(Zn_{1/3}B_{2/3}{}^{5+})_xTi_{1-x}O_2$ (B^{5+} = Nb, Ta) ceramics were decreased with $Zn_{1/3}B_{2/3}{}^{5+}O_2$ content due to the decrease of cation rattling and the distortion of oxygen octahedral, respectively. For the same content of $Zn_{1/3}B_{2/3}{}^{5+}O_2$, K and *TCF* of the specimens with $Zn_{1/3}Ta_{2/3}O_2$ were smaller than that of the specimens with $Zn_{1/3}Nb_{2/3}O_2$. *Qf* value of specimens with $Zn_{1/3}Nb_{2/3}O_2$ showed smaller value than those of the specimens with $Zn_{1/3}Ta_{2/3}O_2$ due to the reduction of Ti ion. Typically $K = 55.3$, $Qf = 17{,}500$ GHz, $TCF = 29.9$ ppm/°C was obtained for $(Zn_{1/3}Ta_{2/3}{}^{5+})_{0.70}Ti_{0.30}O_2$ specimens sintered at 1200 °C for 3 h.

Acknowledgement

This work was supported by the Korea Research Foundation Grant funded by the Korean Government (MOEHRD) (KRF-2006-311-D00527).

References

[1] I.M. Reany, E.L. Colla, N. Setter, Dielectric and structural characteristics of Ba- and Sr-based complex perovskites as a function of tolerance Factor, Jpn. J. Appl. Phys. 33 (1994) 3984–3990.
[2] J. Andrade, M.E. Villafuerte-Castrejon, R. Valenzuela, A.R. West, Rutile solid solutions containing M^+ (Li), M^{2+} (Zn, Mg), M^{3+} (Al) and M^{5+} (Nb, Ta, Sb) ions, J. Mater. Sci. Lett. 5 (1986) 147–149.
[3] R.D. Shannon, Revised effective ionic radii and systematic studies of interatomic distances in halides and chalcogenides, Acta Crystallogr. A32 (1976) 751–767.
[4] S.D. Mo, W.Y. Ching, Electronic and optical properties of three phases of titanium dioxide: rutile, anatase, and brookite, Phys. Rev. B 51 (19) (1995) 13023–13032.
[5] B.W. Hakki, P.D. Coleman, A dielectric resonator method of measuring inductive capacities in the millimeter range, IRE Trans. Microwave Theory Tech. MTT18 (1970) 476–485.
[6] T. Nishikawa, K. Wakino, H. Tamura, H. Tanaka, Y. Ishikawa, Precise measurement method for temperature coefficient of microwave dielectric resonator material, in: IEEE MTT-S International Microwave Symposium Digest, 1987, 277–280.
[7] J.W. Choi, R.B. van Dover, Correlation between temperature coefficient of resonant frequency and tetragonality ratio, J. Am. Ceram. Soc. 89 (3) (2006) 1144–1146.
[8] J.A. García, M.E. Villafuerte-Castrejón, J. Andrade, R. Valenzuela, A.R. West, New rutile solid solutions, $Ti_{1-4x}Li_xM_{3x}O_2$: M = Nb, Ta, Sb, Mater. Res. Bull. 19 (1984) 649–654.
[9] D.W. Kim, D.Y. Kim, K.S. Hong, Phase relations and microwave dielectric properties of $ZnNb_2O_6$–TiO_2, J. Mater. Sci. 15 (6) (2000) 1331–1335.
[10] S.C. Abrahams, J.L. Bernstein, Rutile: normal probability plot analysis and accurate measurement of crystal structure, J. Chem. Phys. 55 (7) (1971) 3206–3211.
[11] W.H. Baur, A.A. Khan, Rutile-type compounds IV. SiO_2, GeO_2 and a comparison with other rutile-type structures, Acta Crystallogr. Section B: Struct. Sci. B27 (1971) 2133–2139.
[12] R.D. Shannon, Dielectric polarizabilities of ions in oxides and fluorides, J. Appl. Phys. 73 (1) (1993) 348–366.
[13] R. Ubic, I.M. Reaney, Structure and dielectric properties of lead pyrochlores, J. Am. Ceram. Soc. 85 (10) (2002) 2472–2478.
[14] N. Michiura, T. Tatekawa, Y. Higuchi, H. Tamura, Role of donor and acceptor ions in the dielectric loss tangent of $(Zr_{0.8}Sn_{0.2})TiO_4$ dielectric resonator material, J. Am. Ceram. Soc. 78 (3) (1995) 793–796.
[15] T. Hirata, Oxygen position, octahedral distortion, and bond-valence parameter from bond lengths in $Ti_{1-x}Sn_xO_2$ ($0 \leq x \leq 1$), J. Am. Ceram. Soc. 83 (12) (2000) 3205–3207.